Proceedings of the XVII ECSMGE-2019
Geotechnical Engineering foundation of the future
ISBN 978-9935-9436-1-3

doi: 10.32075/17ECSMGE-2019-0811

XVII European Conference
ECSMGE 2019
Reykjavik
on Soil Mechanics
and Geotechnical Engineering

Performance and modelling of road embankment supported on rigid inclusions and a transfer platform with steel geogrid

Performance et modélisation du remblai routier supporté par des inclusions rigides et d'une plate-forme de transfert renforcée avec des géogrilles en acier

M. Topolnicki, G. Sołtys, T. Brzozowski
Keller Polska, Gdańsk, Poland

ABSTRACT: Foundation design of about 6 m high road embankment, crossing up to 15 m thick deposits of soft organic soils. The constrains to the project caused by poor ground conditions and a high groundwater level were overcome using a combination of Controlled Stiffness Columns (CSC) and a Load Transfer Platform (LTP) incorporating steel geogrid reinforcement. The LTP was employed to transfer the embankment loads via arching to a grid of CSCs, which further transferred the loads through soft soils to the underlying moraine clays and sands, while the geogrid, capable of taking significant spreading forces with limited elongation, was used to prevent outer CSCs from excessive horizontal displacements and bending. A monitoring system, installed in a representative cross-section and maintained for more than 4-years, allowed observation of vertical and horizontal deformations of the embankment, elongation of the geogrid, and vertical stresses acting on the columns and on the soil in-between. Selected back analyses using 3D and 2D FE models were conducted to compare calculations with the measurements, illustrating capacity and limitations of current design practice.

RÉSUMÉ: Conception des fondations d'un remblai routier de 6 m de hauteur, traversant jusqu'à 15 m d'épaisseur de dépôts de sols organiques meubles. Les contraintes imposées par projet par les conditions de sol médiocres et la nappe phréatique élevée ont été surmontées grâce à une combinaison de colonnes à rigidité contrôlée (CSC) et d'une plate-forme de transfert de charge (LTP) incorporant un renforcement en acier de treillis soudés. La platef-forme a été utilisé pour transférer les charges de remblai en mobilisant l'effet d'arche vers le maillage de CSC, qui a ensuite transféré les charges à travers des sols mous vers les argiles et les sables de moraine sous-jacents. Tandis que la géogrille, capable de supporter d'importantes forces de d'étirement avec un allongement limité, était utilisée afin d'empêcher les CSC au pied du remblai de se déplacer horizontalement et de se plier excessi-vement. Un propre système de surveillance, installé dans une section représentative et fonctionnant depuis plus de 4 ans, a permis d'observer les déformations verticales et horizontales du remblai, l'allongement de la treillis et les contraintes verticales agissant sur les colonnes et le sol entre les deux. Une sélection d'analyses rétrospec-tives utilisant des modèles MEF 3D et 2D ont été menées pour comparer les résultats de calculs avec les mesures, illustrant la capacité et les limites de la pratique de conception.

Keywords: road embankment, rigid inclusions, CSC columns, steel geogrid, monitoring, FE modelling

1 INTRODUCTION

A bypass road near Stawiski along the S-61 national carriageway in Poland included a new bridge to be built over a small river and animal crossing (Figure 1 and 2). The access embankments on both sides of the bridge, up to about 6 m high, had to be constructed on deep deposits of very soft organic soils.

The adopted foundation system, designed and built in 2013, comprised rigid inclusions (Controlled Stiffness Columns) with a diameter of 360 mm and up to 19.5 m long, arranged in a rectangular grid with 1.4 to 2.2 m c/c side spacing. The CSCs were made of unreinforced concrete class C16/20, with the exception of two outer column rows on both sides of each embankment which were additionally reinforced with 12 m long steel beams type IPE 160 to accommodate bending moments and shearing forces resulting from embankment's lateral displacements.

Above the CSC columns a Load Transfer Platform (LTP) was constructed, comprising a single geogrid made of galvanized steel mesh. The geogrid was positioned 30 cm above the column heads and was composed of steel rods, 10 mm in diameter, arranged in a 100×130 mm c/c mesh (smaller distance perpendicular to road axis). The individual geogrid segments, 2.4 m wide and about 5 to 10 m long, were connected with steel hooks along the embankment's longitudinal direction, while in the transverse direction they were laid down with an overlap of 1.6 m. The LTP layer was constructed using the same sand/gravel fill material as used for both access embankments.

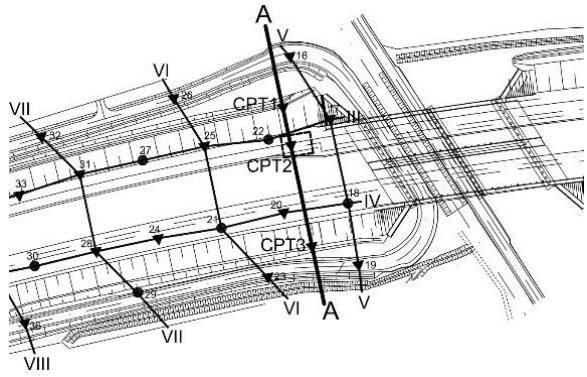

Figure 2. Plan view of the construction site and the location of CPTs and the monitored cross-section A-A

In spite of the increasingly frequent use of rigid inclusions in combination with reinforced LTPs for foundation of embankments on soft soils, in most projects single or multiple layers of geosynthetic reinforcement have been typically applied. In case of welded steel mesh used for the same purpose, the accumulated experience was and is still very limited. Therefore it was decided during construction works to install an inbuilt monitoring system in a representative cross-section of the embankment (Figure 3). The purpose was to observe the performance of the whole foundation system and its key structural elements during construction and operational phases, and to collect data enabling verification of the design method and validation of the foundation system used for the benefit of future similar projects.

Figure 1. The S-61 national carriageway near Stawiski in Poland.

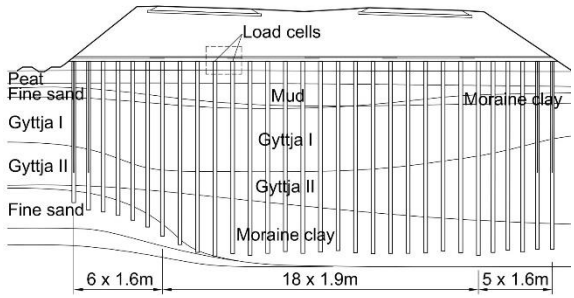

Figure 3. Monitored cross-section A-A and soil stratification (cf. Figure 2).

2 GROUND CONDITIONS

The subsoil consisted of wet peat, mud and gyttja, followed by moraine clays and fine sands. Representative CPTs are shown in Figure 4, and selected parameters of organic soils in Table 1.

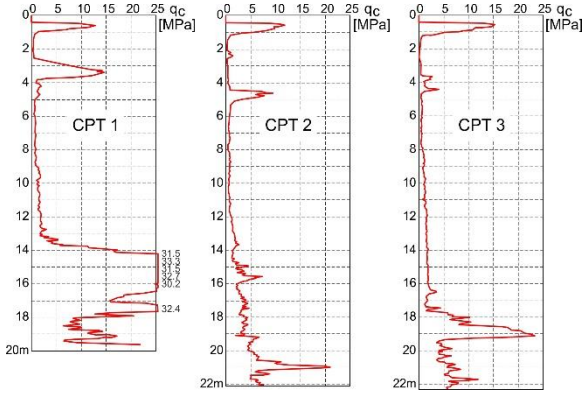

Figure 4. CPTs in the monitored cross-section A-A.

Table 1. Engineering parameters of organic soils

Soil	Cone tip resistance, q_c [MPa]	Shear strength S_u [MPa]	Compress. modulus, $E_{1\%}$ [MPa]	Dilatom. modulus, M_D[MPa]
Peat	0 – 0.5	0 – 20	0.8 – 1.5	1.0
Mud	0.5 – 1	25 – 40	–	1.0 – 2.0
Gytia I	0.2 – 0.8	30 – 50	4 – 20	3 – 30
Gytia II	1.0 – 2.0	50 – 100		

3 INSTALLED INSTRUMENTATION

Focus was on gathering data indicating load distribution between the columns and the ground, vertical and horizontal displacements of the subsoil below the embankment, internal forces and strains in steel geogrid, and on horizontal displacements of CSCs in outer rows as well as of the ground between side columns. To meet these requirements the following instrumentation was installed in the selected location of the embankment and within a square 'unit cell' determined by four CSC columns arranged in a c/c spacing of 1.9 m (Figure 5):

- 4 vertical inclinometers; 2 inside two CSC columns in the outer row (I1 and I2), 2 in the ground between these columns (Figure 6),
- 6 load cells with a diameter of 230 mm; cells C1 and C2 measured compressive stress acting on two column heads, while C3 to C6 ground stress between the columns at the head level (Figure 7),
- 4 horizontal extensometers, attached to steel geogrid for measuring resultant grid elongation including overlapping, whereby sensors E1 to E3 were spanned across three grid segments and E4 over two grid segments (Figure 8),
- 2 flexible tubes, placed in the fill 30 to 50 cm above the geogrid and used to measure settlement along the entire embankment width using specially constructed differential pressure probe pulled throughout the casing (Figure 9).

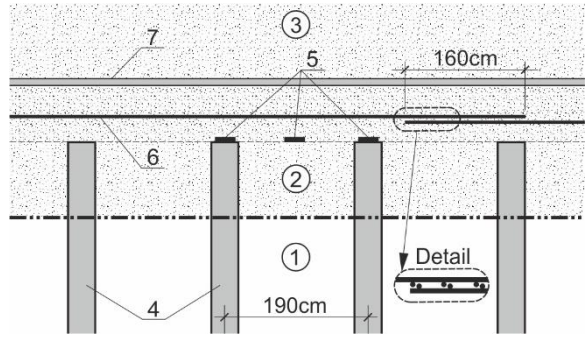

Figure 5: Scheme of instrumentation installed in the monitored cross-section: (1) soft soil, (2) working platform, (3) embankment fill, (4) CSCs, (5) load cells, (6)steel geogrid, (7) flexible tube for settlement measurement.

Special sensors to measure local strain in individual rods of the geogrid were also installed, but

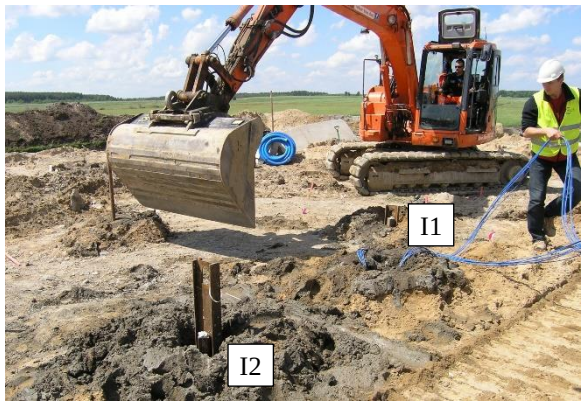

Figure 6: Installation of inclinometers along the outer row of CSCs.

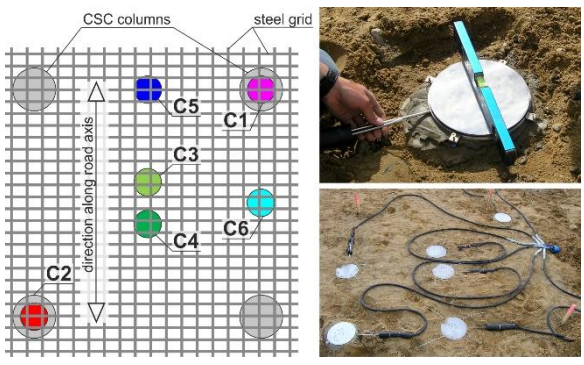

Figure 7: Location of load cells on column heads and on the ground.

Figure 8. Special system to measure elongation of steel geogrid including overlaps (Wilde Engineering).

were incidentally overstressed during compaction of bottom embankment layers with heavy rollers and their readings could not be reliably evaluated. Monitoring was continued with varying frequency during construction and operational phases, while selected readings could be taken even about 4.5 years after system installation.

Figure 9. Measurement of settlement using differential pressure probe inserted into a flexible tube and pulled across the embankment (Wilde Engineering).

4 FINITE ELEMENT MODELLING

The purpose of numerical modelling was to check by means of back analyses and comparisons with measurements to what extent commercially available software packages, which are typically used in engineering practice, can be used to responsibly design similar foundation systems. Therefore only the available constitutive models and modelling options provided in the selected software package were utilised, and no attempt was made for a more advanced modelling. Consequently, the following two FE models have been applied for the numerical study:

- a general 3D model, which represented embankment section and ground conditions at the location of monitoring instruments, developed using PLAXIS 3D modelling capacity (Figure 10),
- a unit cell model, representing single column and the surrounding soil, developed in axisymmetric space using PLAXIS 2D (Figure 11).

The modelled section of the embankment in the 3D representation included three rows of CSC columns, whose lengths were derived from automated readings of the piling rig. The arrangement of soil layers corresponded to the profile shown in Figure 3, and was kept constant across the model 'thickness'. The CSCs were modelled as linear elastic beam elements with embedded interface elements to describe the interaction with the soil along column shaft and at the base. Steel geogrid was modelled with elasto-plastic shell element with no bending stiffness, but allowing for anisotropic stiffness of the steel mesh in both main directions of elongation. The adopted FE mesh included about 136,000 of tetrahedral elements with 10-nodes.

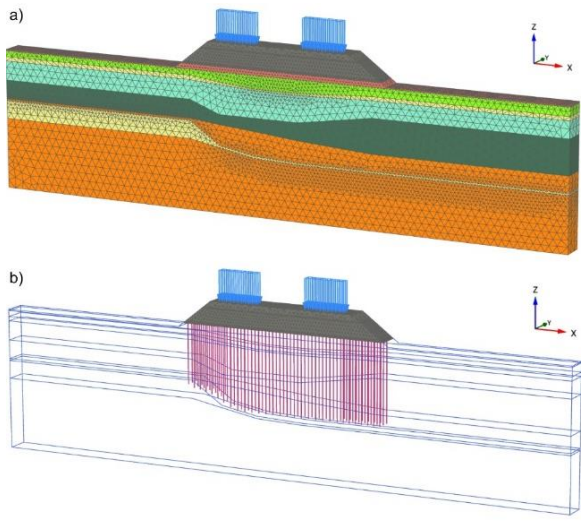

Figure 10. The general model, (a) 3D mesh, (b) CSCs modelled as embedded beam elements.

The unit cell model was established to allow better representation of local phenomena associated with arching mechanism around the column head using very fine FE mesh, leading to more adequate load distribution between the column, the surrounding ground, and the geogrid. In this case the CSC column was modelled with volumetric (or soil type) elements with linearly elastic material properties to represent concrete. Interface elements enabling reduction of ground strength and stiffness along the column shaft have been also used. To account for large relative displacements between the column and the soil, especially around column's head, continuous updating of the shape of FE elements was activated by selecting the "updated mesh" option in PLAXIS 2D. The soil profile corresponded to CPT2.

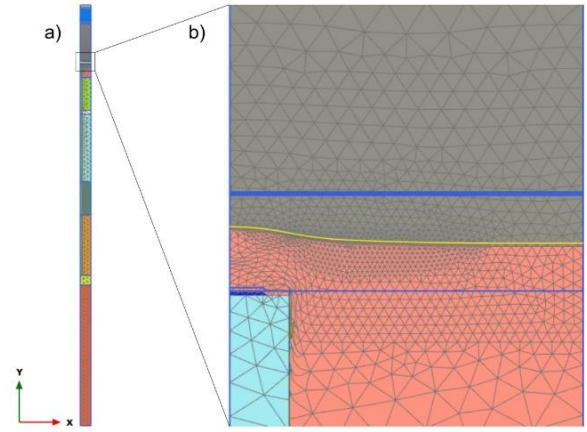

Figure 11. The unit cell model, (a) unit cell in axisymmetric space, (b) FE mesh around column head.

In both FE models the same soil parameters were used, and the stress-strain relationship was represented with the Hardening Soil constitutive model. Embankment construction was modelled stepwise and with account for ground consolidation. Following the installation of rigid inclusions and monitoring system, the first phase of embankment construction to the height of 5.1 m took 18 days. Because of other works at the nearby bridge abutment, the height of 5.4 m was reached after 101 days, and the final height of 5.69 m over the next 23 days. The operational phase began 142 days after construction onset, and was modelled with a uniform live loading of 25 kPa, applied on both road lanes.

5 OBSERVED AND COMPUTED BEHAVIOUR

Figure 12 shows observed and computed vertical stress acting on the column head and in the

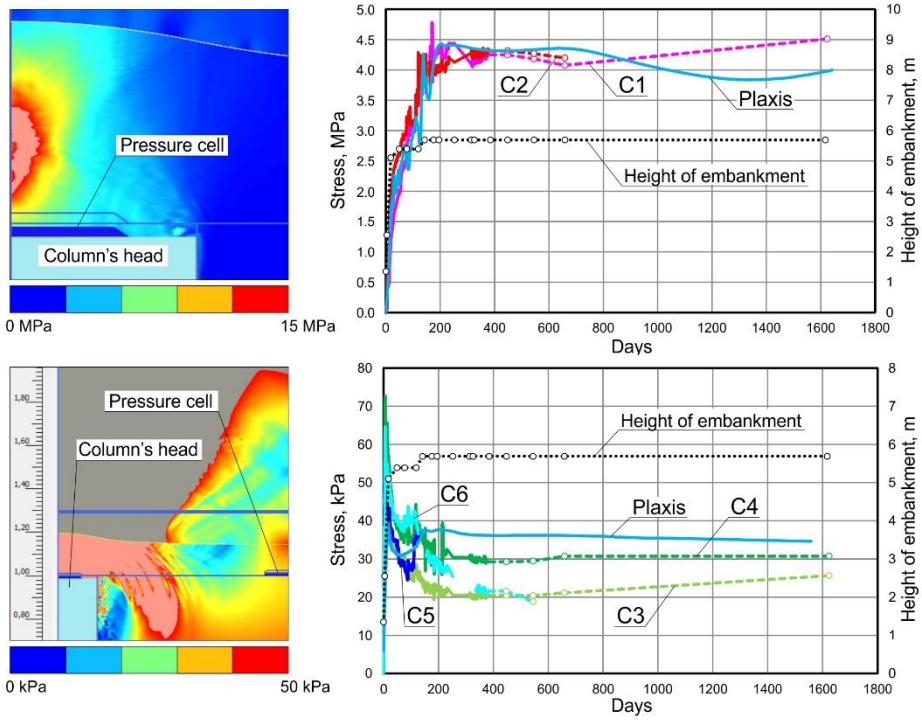

Figure 12. Vertical stress distribution around column head computed with the unit cell model for t_e=1642 days, and stresses recorded with load cells in comparison with computed stress development in time; C1 and C2 – load cells above column heads, C3 to C6 – load cells placed on the ground (for detail location see Figure 7).

ground, obtained with the unit cell model. In addition to stress distribution figures which illustrate significant stress variation across the selected cell sections, the average computed stresses acting on the load cells in time have been calculated and plotted together with the data recorded during monitoring. In both cases a satisfactory agreement has been obtained, corroborating capacity of the axisymmetric FE model to reproduce complex arching behaviour in LTP systems. Furthermore, field measurements have not shown any decrease of the supportive ground pressure in time despite the presence of very soft organic soil directly below the working platform.

The computed and observed settlements in the reference cross-section of the full embankment are depicted in Figure 13. The maximum settlement calculated in the vertical plane between the columns was 198 mm, and the largest increase of settlement during the operational phase at the level of the embankment crest was 15 mm, well below the allowable limit of 30 mm. In addition, an attempt was made to compare the calculated and measured vertical displacements along the line defined by the measuring tubes shown in Figure 9, noting that the steel geogrid was unintentionally rotated about 4.5° in relation to the column arrangement, as shown in Figure 13b. Although the computed and measured curves show a satisfactory coincidence in terms of maximum and minimum values (estimated accuracy of measurements is about 5 mm), the course of observed deformation could not be fully reproduced along the whole embankment section, and especially between 32 and 50 m of embankment's width. The reason for this discrepancy has not been clearly explained. One can only expect that the elongated columns in this region should have higher axial stiffness than in the adopted FE model.

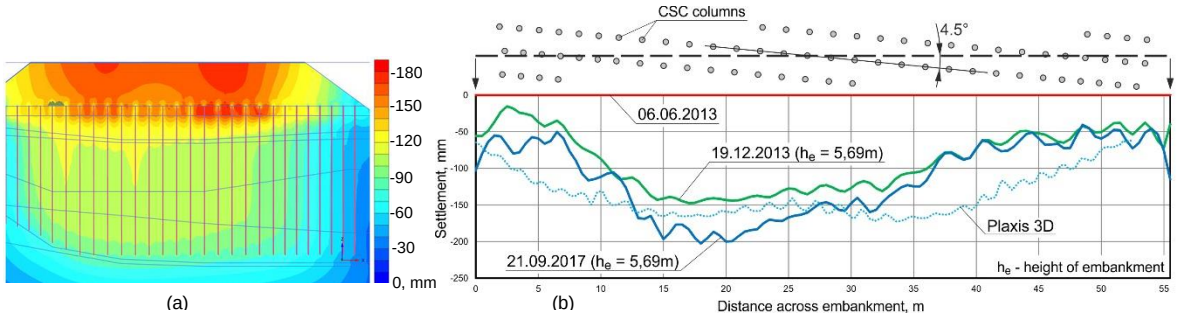

Figure 13. Computed and observed settlement during monitoring period; (a) settlement in the vertical plane across the central row of columns in the 3D model, (b) observed and computed settlement along the line of measurement: Red – commencement of measurements, Green – end of construction, Blue – end of monitoring.

Figure 14 shows tensile forces in the steel geogrid and the vertical displacements at the geogrid level, computed with the 3D model. The maximum calculated tensile force along the main direction of grid elongation was 229 kN/m, and the maximum differential deflection of the geogrid was 26 mm. The measurements conducted with specially built extensometers, spanned across geogrid segments to include the effect of overlapping, yielded about 250 kN/m (Figure 15).

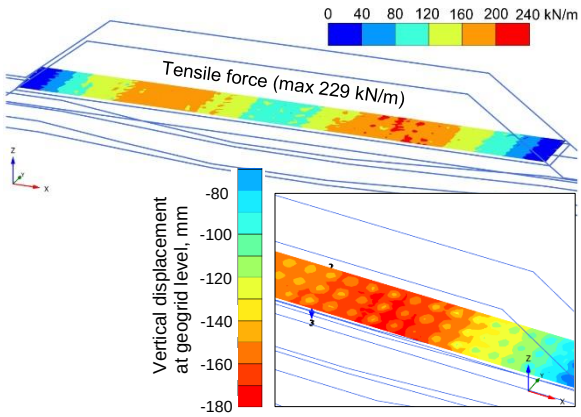

Figure 14. Tensile force in the geogrid and settlement at the geogrid level, obtained with the 3D model.

A more detailed numerical study using the unit cell model has shown that maximum differential deflection of the geogrid can reach 68 mm, as shown in Figure 16, leading to a greater tensile force of about 280 kN/m (with local plastification occurring above the column head). This example

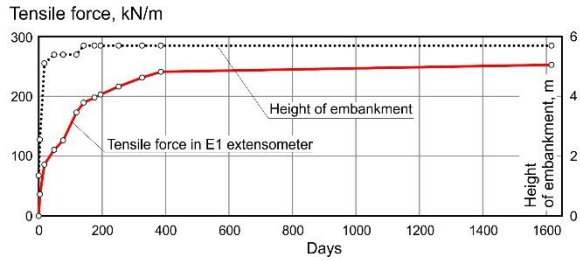

Figure 15. Observed tensile force in steel geogrid based on the reading of extensometer E1.

demonstrates that spatial FE models used in current design practice may undervalue the tensile forces in the geogrid because of inherent modelling constrains. This disadvantage can be overcome by the parallel application of the axisymmetric model.

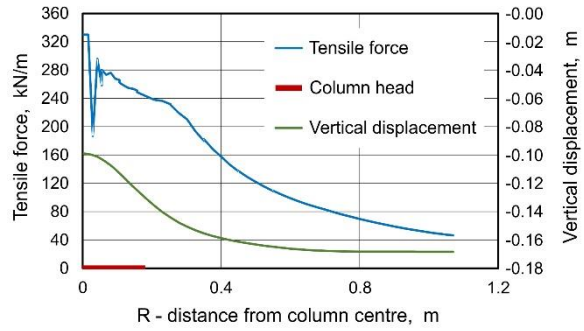

Figure 16. Vertical displacement and tensile force in steel geogrid obtained with the unit cell model.

The horizontal displacements of the outer row of CSC columns have been computed with the 3D

model with a varying accuracy (Figure 17). The maximum deflection at the head level closely matches both measurements, but the course of deflection could not be fully reproduced. The obtained difference could not be explained.

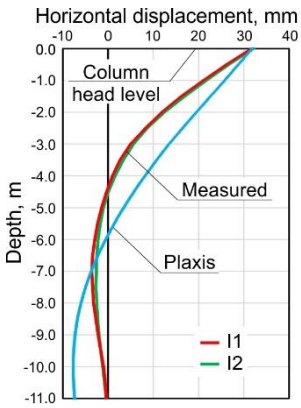

Figure 17. Observed and computed horizontal displacement of two CSCs located in outer row.

6 CONCLUSIONS

The described road embankment, operated since 2014, behaves as anticipated, with no excessive vertical and horizontal displacements or differential settlements. This confirms the legitimacy of the implemented solution, whose basic elements are rigid inclusions and the transmission layer reinforced with a steel geogrid, which is of fundamental importance for effective limitation of horizontal displacements of high embankments quickly constructed on a soft ground.

Limited experience in the design of similar structures prompted the authors to perform field investigations and numerical analysis in relation to collected measurements, assuming the use of commercially available FE software commonly applied in the engineering practice. The conducted back analyses using suitably developed 3D and 2D models confirmed, in our opinion, the possibility of prediction of deformations and internal forces in all elements of the adopted foundation system with an accuracy sufficient for practical design, provided appropriate parameters and modelling techniques are used, including a controversial application of a shell element for modelling of a steel geogrid (what should be compensated with appropriately adopted safety factors).

An accurate prediction of tensile forces in the reinforcement embedded in load transfer layers using numerical models, even if restricted to more frequently used geosynthetics, represents still a challenging task despite numerous research studies. In some regulations, such as e.g. CUR'2016, the use of numerical models for determination of forces in basal reinforcements has been banned in favour of the analytical methods. Without prejudging the introduction of such principles in the regulations, it can be demonstrated with reference to the considered case study that the application of the CUR'2016 method, for instance, would lead to a significant increase of the calculated tensile force. Assuming that the subgrade reaction is about 30/0.068=440 kN/m^3 based on the data shown in Figures 12 and 16, the resulting characteristic tensile force is 748 kN/m.

In addition, the principle of adding tensile forces resulting from the effect of reinforcement straining caused by vertical loading (membrane stretching) and by the horizontal trust of the embankment, also recommended in CUR'2016 and BS8006, has not been confirmed in the analyses and measurements carried out.

7 ACKNOWLEDGEMENTS

Gratitude is express to Prof. Krzysztof Wilde and Dr. Mikołaj Miśkiewicz from the Gdańsk University of Technology and Wilde Engineering Ltd. for their contribution in developing the monitoring system and for conducting measurements.

8 REFERENCES

CUR'2016, Design Guidelines Basal Reinforced Piled Embankments (CUR226), CRC Press, ISBN 978 90 5367 624 0.